

Measurement of Sixth Cumulant of the Net-Proton Multiplicity Distributions in Au+Au Collisions at

$\sqrt{s_{NN}} = 200$ GeV at the STAR Experiment

STAR

Toshihiro Nonaka, for the STAR Collaboration
University of Tsukuba, CiRFSE



Lattice QCD calculation predicts the phase transition at small μ_B is the smooth crossover. Experimentally, however, there is still no direct evidence for the phase transition. The sixth order cumulant (C_6) is predicted to probe the phase transition, that will be negative at the phase transition. In this poster, the sixth order cumulant (C_6) of net-proton multiplicity distribution has been measured at the extended p_T region ($0.4 < p_T < 2.0$ GeV/c) with efficiency correction in Au+Au collisions in $\sqrt{s_{NN}} = 200$ GeV. Centrality, p_T and rapidity dependence of C_6/C_2 are presented.

Motivation

Smooth crossover at small μ_B predicted by Lattice QCD

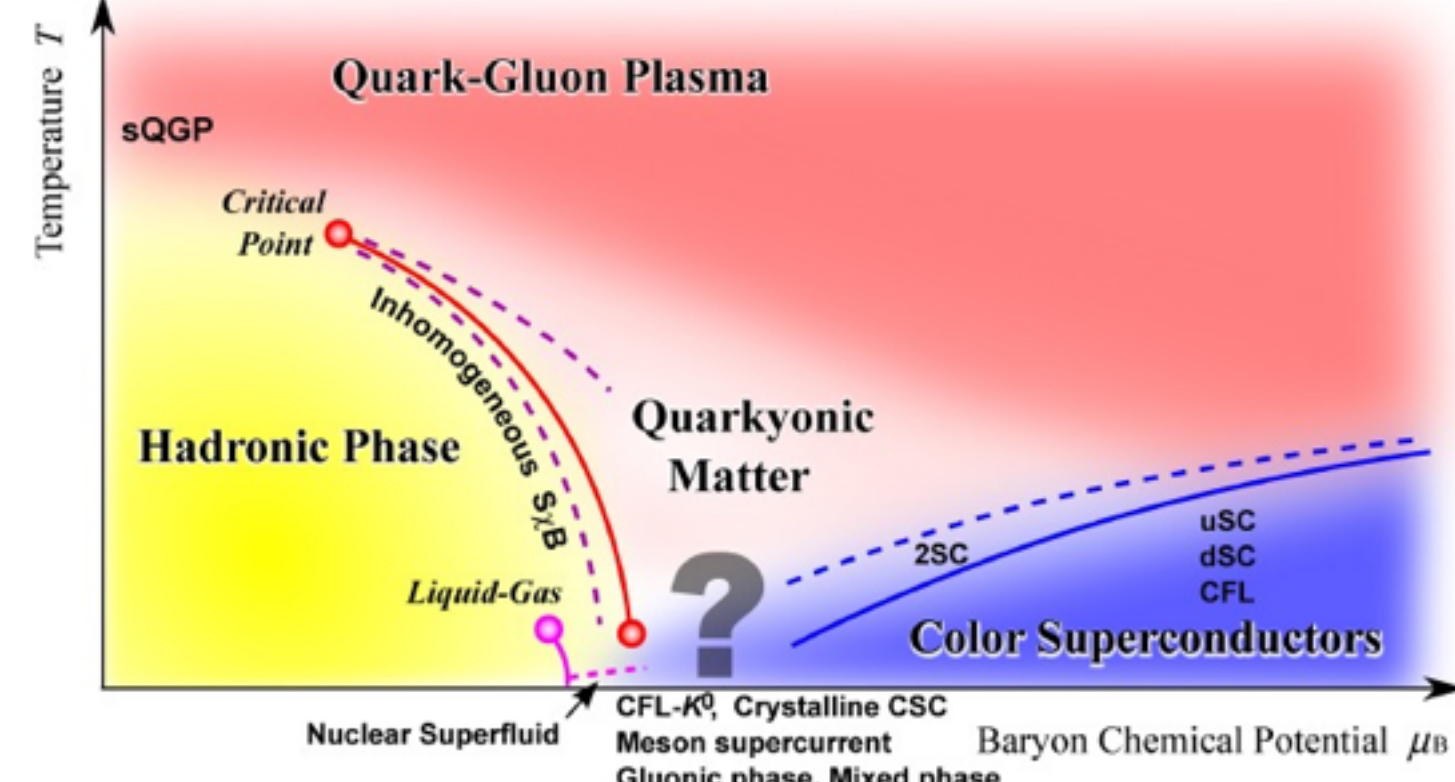
Experimentally no evidence for the phase transition

$C_6 < 0$ (net-baryon or net-charge) predicted at the phase transition

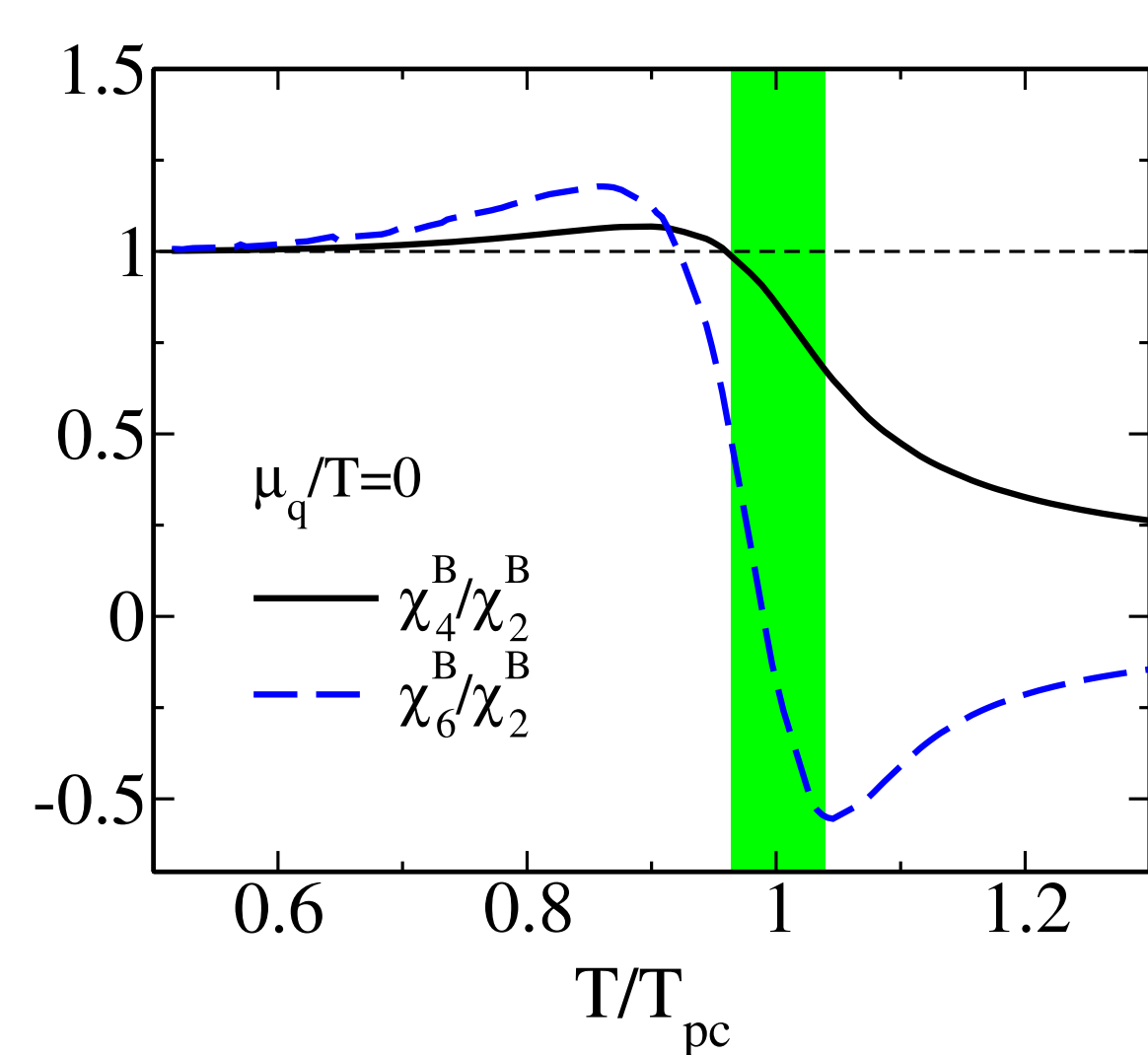
$\frac{C_6}{C_2} = \frac{\chi_6}{\chi_2} \rightarrow$ Cumulant ratio directly connected to the susceptibility

C_6/C_2 of net-proton distribution is measured at $\sqrt{s_{NN}} = 200$ GeV with STAR detector to find the evidence of the phase transition

K. Fukushima and T. Hatsuda, Rept. Prog. Phys. **74**, 014001(2011)



Friman et al, Eur. Phys. J. C (2011) 71:1694



Efficiency correction

- Calculation cost for efficiency correction become large by power of efficiency bins with formulas based on the factorial moments (Bzdak and Koch, 2016), which is crucial for the sixth order cumulant.
- Nonaka, Kitazawa and Esumi developed a new efficiency correction. Calculation cost increases linearly with the number of efficiency bins.
- In addition to the p_T dependence, acceptance non-uniformity in phi direction are corrected.

$$\langle Q^6 \rangle_c = \langle q_{(1,1)}^6 \rangle_c - 15 \langle q_{(1,1)}^4 q_{(2,2)} \rangle_c + 15 \langle q_{(1,1)}^4 q_{(2,1)} \rangle_c - 90 \langle q_{(1,1)}^2 q_{(2,2)} q_{(2,1)} \rangle_c + 40 \langle q_{(1,1)}^3 q_{(3,3)} \rangle_c + 45 \langle q_{(2,2)}^2 q_{(1,1)} \rangle_c + 20 \langle q_{(1,1)}^3 q_{(3,1)} \rangle_c - 60 \langle q_{(1,1)}^3 q_{(3,2)} \rangle_c + 45 \langle q_{(1,1)}^2 q_{(2,1)}^2 \rangle_c - 90 \langle q_{(1,1)}^2 q_{(4,4)} \rangle_c - 120 \langle q_{(3,3)} q_{(2,2)} q_{(1,1)} \rangle_c - 15 \langle q_{(3,2)}^2 \rangle_c + 15 \langle q_{(1,1)}^2 q_{(4,1)} \rangle_c - 60 \langle q_{(1,1)} q_{(2,2)} q_{(3,1)} \rangle_c - 60 \langle q_{(1,1)}^2 q_{(4,2)} \rangle_c + 120 \langle q_{(1,1)} q_{(2,1)} q_{(3,3)} \rangle_c + 180 \langle q_{(1,1)}^2 q_{(4,3)} \rangle_c + 45 \langle q_{(2,2)}^2 q_{(2,1)} \rangle_c + 180 \langle q_{(1,1)} q_{(2,2)} q_{(3,2)} \rangle_c - 45 \langle q_{(1,1)}^2 q_{(4,2)} \rangle_c - 45 \langle q_{(2,1)}^2 q_{(2,2)} \rangle_c - 180 \langle q_{(1,1)} q_{(2,1)} q_{(3,2)} \rangle_c + 60 \langle q_{(1,1)} q_{(2,1)} q_{(3,1)} \rangle_c + 15 \langle q_{(2,1)} \rangle_c + 144 \langle q_{(5,5)} q_{(1,1)} \rangle_c + 90 \langle q_{(4,4)} q_{(2,2)} \rangle_c + 40 \langle q_{(3,3)}^2 \rangle_c + 6 \langle q_{(5,1)} q_{(1,1)} \rangle_c + 15 \langle q_{(4,1)} q_{(2,1)} \rangle_c + 10 \langle q_{(3,1)}^2 \rangle_c - 30 \langle q_{(5,2)} q_{(1,1)} \rangle_c - 15 \langle q_{(4,1)} q_{(2,2)} \rangle_c + 300 \langle q_{(5,3)} q_{(1,1)} \rangle_c + 40 \langle q_{(3,3)} q_{(3,1)} \rangle_c + 60 \langle q_{(4,2)} q_{(2,2)} \rangle_c - 360 \langle q_{(5,4)} q_{(1,1)} \rangle_c - 90 \langle q_{(4,4)} q_{(2,1)} \rangle_c - 120 \langle q_{(3,3)} q_{(3,2)} \rangle_c - 180 \langle q_{(4,3)} q_{(2,2)} \rangle_c + 180 \langle q_{(4,3)} q_{(2,1)} \rangle_c + 45 \langle q_{(4,2)} q_{(2,2)} \rangle_c + 90 \langle q_{(3,2)}^2 \rangle_c - 60 \langle q_{(3,2)} q_{(3,1)} \rangle_c - 60 \langle q_{(4,2)} q_{(2,1)} \rangle_c - 60 \langle q_{(5,2)} q_{(1,1)} \rangle_c - 45 \langle q_{(4,2)} q_{(2,1)} \rangle_c - 120 \langle q_{(6,6)} \rangle_c + 360 \langle q_{(6,5)} \rangle_c - 390 \langle q_{(6,4)} \rangle_c + 180 \langle q_{(6,3)} \rangle_c - 31 \langle q_{(6,2)} \rangle_c + \langle q_{(6,1)} \rangle_c$$

M : # of efficiency bins
 n : # of particles
 p : efficiency
 a : electric charge

$$q_{(r,s)} \equiv \sum_{i=1}^M \frac{a_i^r}{p_i^s} n_i$$

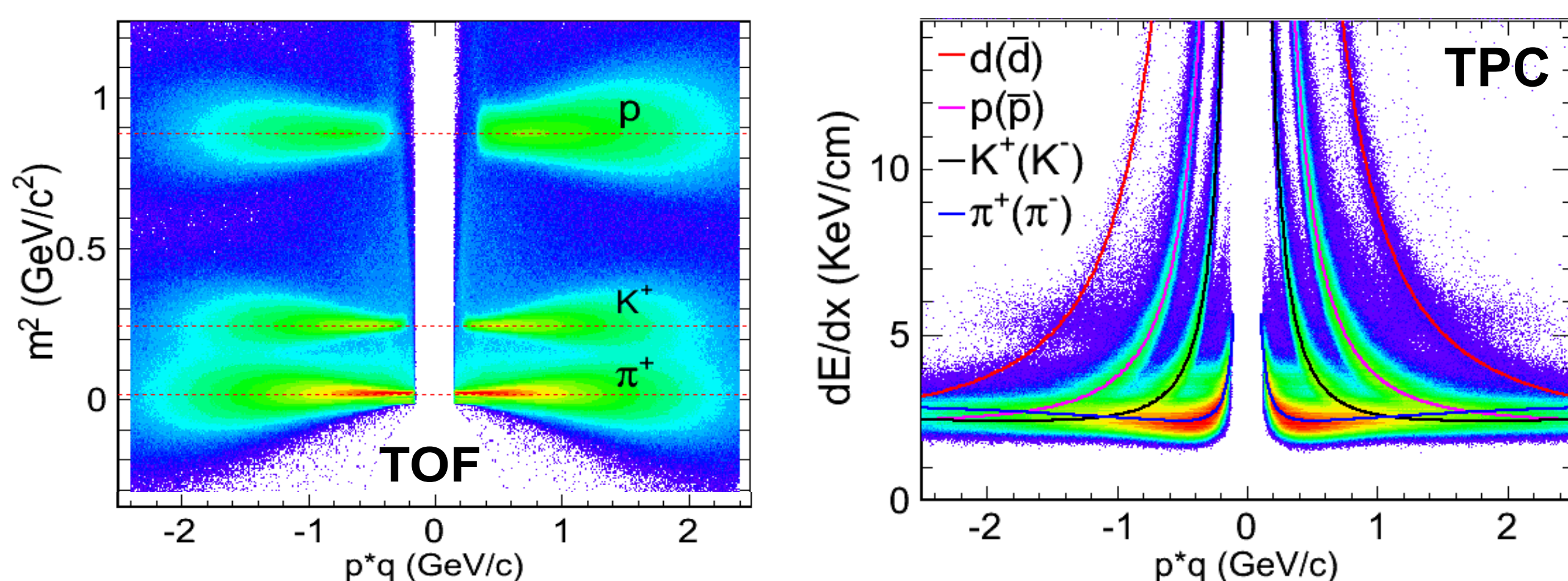
\rightarrow Nonaka, Kitazawa and Esumi: in preparation

Analysis techniques

X. Luo and N. Xu, arXiv: 1701.02105

Proton identification

- Large and uniform acceptance with full azimuthal angles with $|\eta| < 1.0$
- At low p_T region ($0.4 < p_T < 0.8$ GeV/c) dE/dx measured by TPC is used.
- At high p_T region ($0.8 < p_T < 2.0$ GeV/c) combined PID with TOF is implemented.



Centrality determination

- Use charged particles except protons in order to avoid the auto-correlation.

Centrality bin width correction

- Calculate cumulants at each multiplicity bin and average them in one centrality, which leads to the suppression of the volume fluctuation.

Statistical errors: Bootstrap

- Make a new distribution by random sampling from the original net-proton distribution and calculate cumulants.
- This procedure is repeated with 300 times, and the statistical errors are taken from the RMS of the cumulants.

Summary

- \rightarrow We present high statistics results of centrality, p_T and rapidity dependence of C_6/C_2 of net-proton multiplicity distributions from $\sqrt{s_{NN}} = 200$ GeV in Au+Au collisions.
- \rightarrow Results are consistent with zero within 2σ with current statistics.

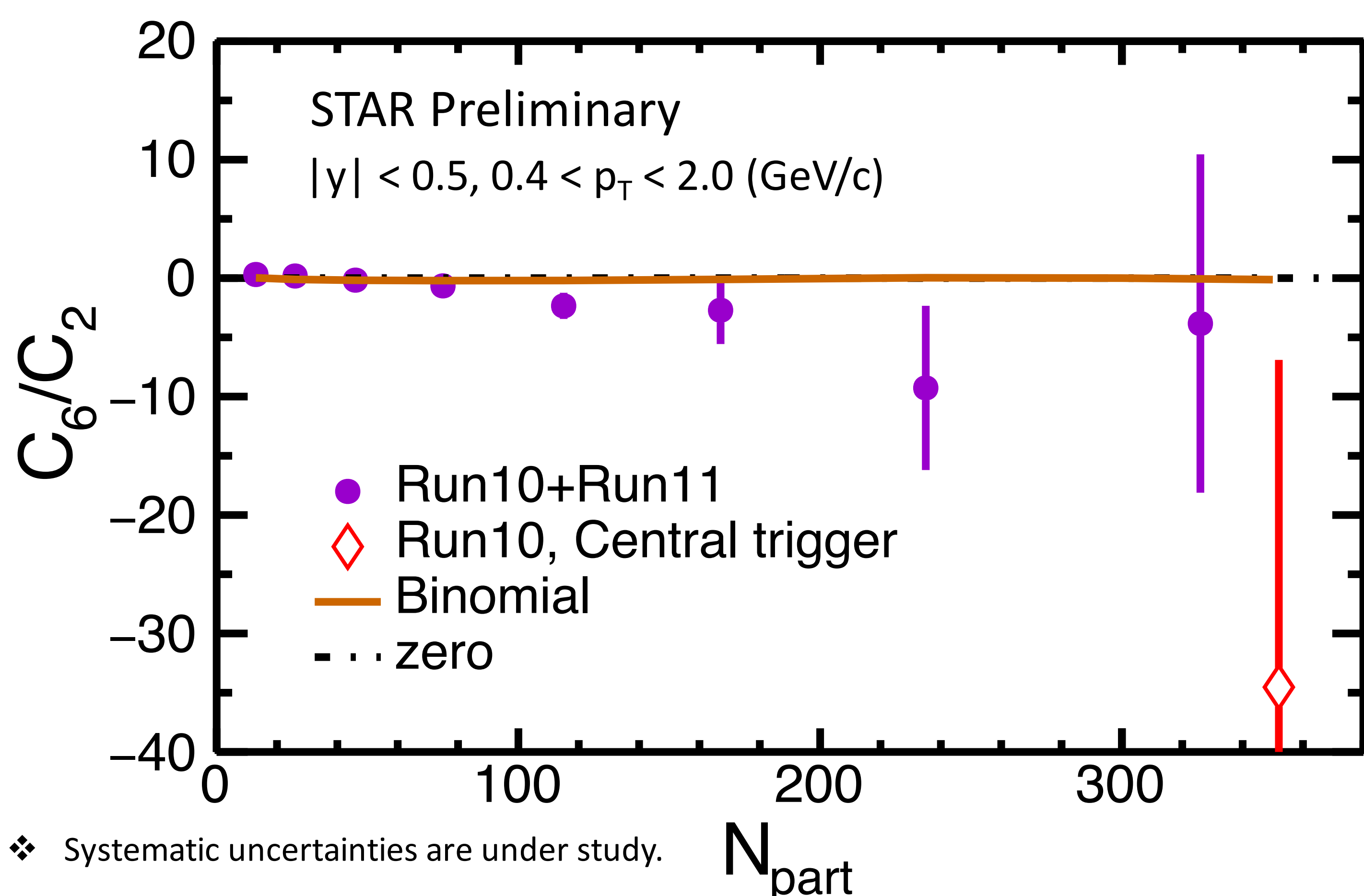
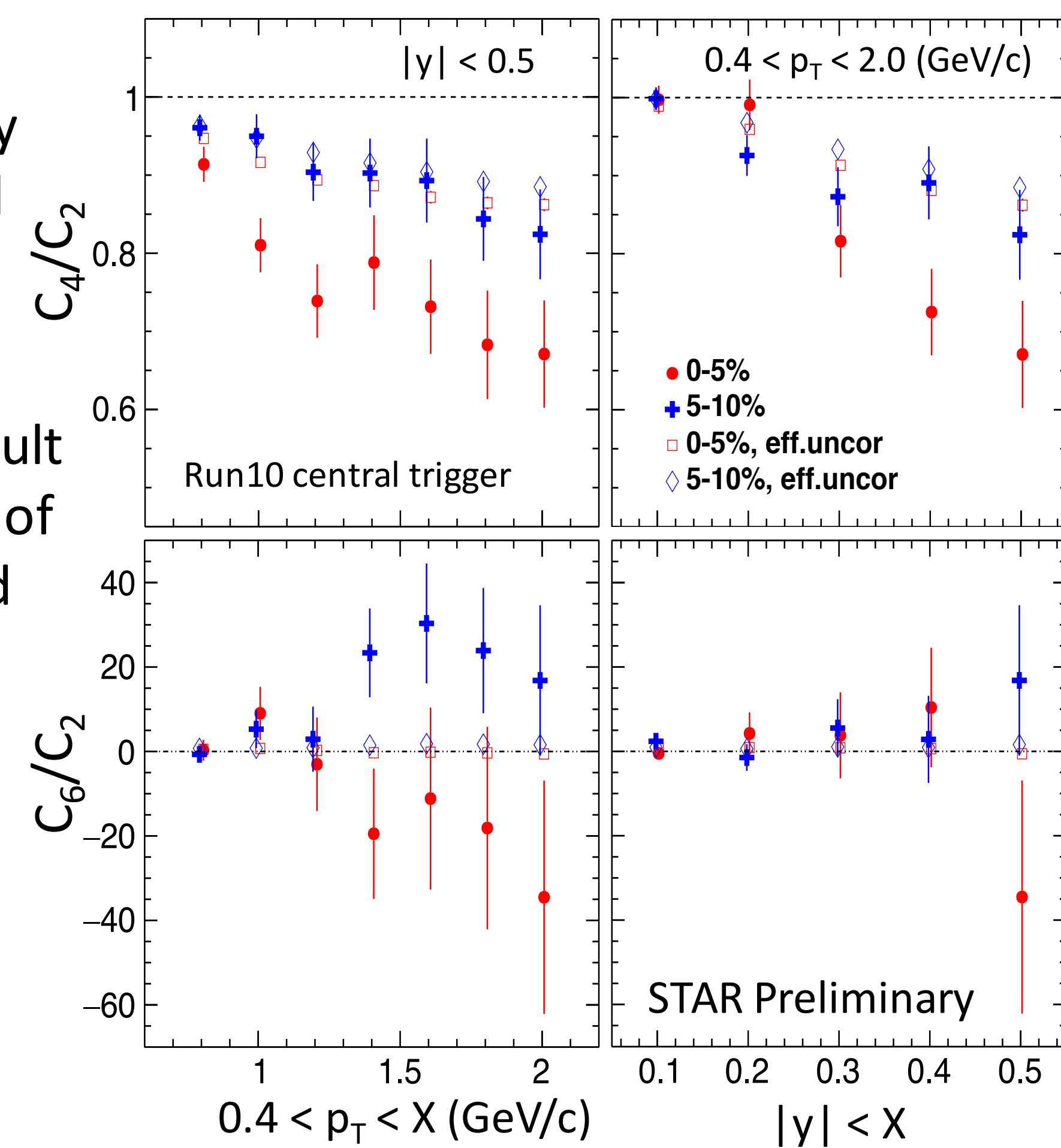
Results

- \rightarrow (Right plot) p_T and rapidity dependence of C_4/C_2 and C_6/C_2 at central collisions.

- \rightarrow (Bottom plot) Merged result of centrality dependence of C_6/C_2 between Run10 and Run11.

✓ Used statistics

	0-10%	10-80%
Run10	~160M	~200M
Run11	~50M	~450M



Systematic uncertainties are under study.